Vibrational, Electronic, and Resonance Raman Spectral Studies of $[Cu_2(XYL-O-)O_2]^+$, a Copper(II) Peroxide Model Complex of Oxyhemocyanin

James E. Pate,[†] Richard W. Cruse,[‡] Kenneth D. Karlin,*[‡] and Edward I. Solomon*[†]

Contribution from the Departments of Chemistry, Stanford University, Stanford, California 94305, and State University of New York at Albany, Albany, New York 12222.
Received August 21, 1986

Abstract: Spectroscopic studies have been performed on $[Cu_2(XYL-O-)O_2]^+$ to determine the geometric and electronic structure of peroxide binding in this complex. The charge-transfer spectrum shows a band at 505 nm (ϵ = 6300 M^{-1} cm^{-1}) with a weaker shoulder near 610 nm (ϵ = 2400 M^{-1} cm^{-1}). Resonance Raman results indicate the presence of two enhanced vibrations, the copper peroxide stretch at 488 cm^{-1} (464 cm^{-1} using $^{18}O_2$) and the intraperoxide stretch at 803 cm^{-1} (750 cm^{-1} with $^{18}O_2$). The intensity of the intraperoxide stretch shows significant enhancement from both charge-transfer bands. However, the copper peroxide stretch is primarily in resonance with the higher energy transition. Oxygenation with an $^{16}O^{18}O$ mixture indicates that the peroxide is asymmetrically bound, since the copper peroxide stretch is split into two components at 465 and 486 cm^{-1}. These vibrational data have been used for a normal coordinate analysis of the factors determining the mixed isotope splitting of a terminally bound peroxide. These results are then extended to a μ-1,2 geometry, and correlations have been made to the observed spectral features in oxyhemocyanin.

There has been considerable interest in defining the geometric and electronic structure of the coupled binuclear copper active site in hemocyanin.[1] The function of this site is the reversible binding of dioxygen, which occurs from the deoxy form consisting of two copper(I)'s. The resulting oxyhemocyanin exhibits a number of unique electronic spectral features. The electronic absorption spectrum shows an intense band near 345 nm (ϵ = 20000 M^{-1} cm^{-1}) with an additional feature at 580 nm (ϵ = 1000 M^{-1} cm^{-1}), while the circular dichroism shows a negative feature near 480 nm ($\Delta\epsilon \sim 2$ M^{-1} cm^{-1}). Resonance Raman experiments have indicated that the dioxygen binds as peroxide[2] with an intraligand stretching frequency of 749 cm^{-1}. A copper peroxide vibration, however, has not been observed.

Thus, oxyhemocyanin formally contains peroxide bound to two copper(II)'s. A met derivative, [Cu(II)Cu(II)], of the oxyhemocyanin active site can be prepared by ligand displacement of the peroxide. Spectral comparison of the met and oxy derivatives demonstrates that the absorption and circular dichroism bands are peroxide to copper(II) charge-transfer transitions. A transition dipole vector coupling (TDVC) model, developed to analyze this charge-transfer spectrum, suggests that the peroxide bridges the two coppers in a symmetric μ-1,2 geometry.[3] The crystal structure of the deoxy form, [Cu(I)Cu(I)], has been determined,[4] but there has not yet been a refined structure of the oxygenated site.[5] However, EXAFS results, which indicate a 3.6-Å copper–copper distance in oxyhemocyanin,[6] and resonance Raman studies[7] with the mixed isotope $^{16,18}O_2$ are consistent with the μ-1,2 peroxide geometry suggested by the TDVC analysis of the charge-transfer spectrum. Alternatively, the possibility has been raised[8] that the lack of an observed mixed isotope splitting of the peroxide stretch could still be consistent with a terminal peroxide geometry, if the mixed isotope splitting associated with this geometry was less than the experimental resolution limit of 3 cm^{-1}.

A number of groups have attempted to develop chemical model systems which mimic the functional and spectroscopic properties of the biological binuclear copper active sites.[9] Two of these complexes reversibly bind dioxygen, and oxygen–oxygen stretching frequencies have been measured (803[10] and 825 cm^{-1} [11]) which are in the range of peroxide stretching frequencies obtained for other transition metal–peroxide complexes (786–929 cm^{-1}).[12,13] One of these systems involves the XYL-O ligand which contains two tridentate groups (each having an amino and two pyridine donors) that are bridged by a *m*-xylyl connecting unit (Figure 1). This system approximates the histidine residues in the hemocyanin active site[4] and is one of a series where the ligand can be systematically varied, causing perturbations in the spectral features of the oxygenated form.[14] In this study, we have used absorption and resonance Raman spectroscopy combined with normal coordinate calculations to determine the geometry and analyze the spectral features of the peroxide bound in the $[Cu_2(XYL-O-)O_2]^+$ complex. These results are then compared with those for oxyhemocyanin to obtain further understanding of the electronic and geometric structure of peroxide bound to the protein active site. In addition, normal coordinate calculations have been used to further interpret the mixed isotope results for oxyhemocyanin.

Experimental Section

The copper(I) precursor $[Cu_2(XYL-O-)]^+$ was prepared and purified as previously described.[10] The gases $^{18}O_2$ (99.13%, Ventron, Alfa Division, Danvers, MA) and $^{16,18}O_2$ (51 atom % ^{18}O, Cambridge Isotope

[†]Stanford University.
[‡]State University of New York at Albany.

(1) (a) Solomon, E. I. *Pure Appl. Chem.* **1983**, *55*, 1069–1088. (b) Solomon, E. I.; Penfield, K. W.; Wilcox, D. E. *Struct. Bonding (Berlin)* **1983**, *53*, 1–57. Solomon, E. I. *Copper Proteins*; Spiro, T. G., Ed.; Wiley: New York, 1981; pp 41–108.
(2) (a) Freedman, T. B.; Loehr, J. S.; Loehr, T. M. *J. Am. Chem. Soc.* **1976**, *98*, 2809–2815. (b) Larrabee, J. A.; Spiro, T. G. *Ibid.* **1980**, *102*, 4217–4223.
(3) Eickman, N. C.; Himmelwright, R. S.; Solomon, E. I. *Proc. Natl. Acad. Sci. U.S.A.* **1979**, *76*, 2094–2098.
(4) (a) Kuiper, K. A.; Gaastra, W.; Beintema, J. J.; van Bruggen, E. F. J.; Schepman, A. M. H.; Drenth, J. *J. Mol. Biol.* **1975**, *99*, 619–629. (b) Gaykema, W. P. J.; Hol, W. G. J.; Vereijen, J. M.; Soeter, N. M.; Bak, H. J.; Beintema, J. J. *Nature (London)* **1984**, *309*, 23–29. (c) van Schaick, E. J. M.; Schutter, W. G.; Gaykema, W. P. J.; Schepman, A. M. H.; Hol, W. G. J. J. *Mol. Biol.* **1982**, *158*, 457–485. (d) Gaykema, W. P. J.; Volbeda, A.; Hol, W. G. J. *Ibid.* **1985**, *187*, 255–275.
(5) Magnus, K. A.; Love, W. E. *J. Mol. Biol.* **1977**, *116*, 171–173.
(6) (a) Brown, J. M.; Powers, L.; Kincaid, B.; Larrabee, J. A.; Spiro, T. G. *J. Am. Chem. Soc.* **1980**, *102*, 4210–4216. (b) Co, M. S.; Hodgson, K. O. *Ibid.* **1981**, *103*, 2094–2098.
(7) Thamann, T. J.; Loehr, J. S.; Loehr, T. M. *J. Am. Chem. Soc.* **1977**, *99*, 4187–4189.
(8) Klotz, I. M.; Duff, L. L.; Kurtz, D. M., Jr.; Shriver, D. F. *Invertebrate Oxygen-Binding Proteins*; Lamy, J., Lamy, J., Ed.; Marcel Dekker: New York, 1981; pp 469–474.
(9) *Biological & Inorganic Copper Chemistry*; Karlin, K. D., Zubieta, J., Eds.; Adenine Press: Guilderland, NY, 1986; Vol. II.
(10) Karlin, K. D.; Cruse, R. W.; Gultneh, Y.; Hayes, J. C.; Zubieta, J. *J. Am. Chem. Soc.* **1984**, *106*, 3372–3374.
(11) Thompson, J. S. *J. Am. Chem. Soc.* **1984**, *106*, 8308–8309.
(12) Barraclough, C. S.; Lawrance, G. A.; Lay, P. A. *Inorg. Chem.* **1978**, *17*, 3317–3322.
(13) Griffith, W. P.; Wickins, T. D. *J. Chem. Soc. A* **1968**, 397–400.
(14) Karlin, K. D.; Haka, M. S.; Cruse, R. W.; Gultneh, Y. *J. Am. Chem. Soc.* **1985**, *107*, 5828–5829.

0002-7863/87/1509-2624$01.50/0

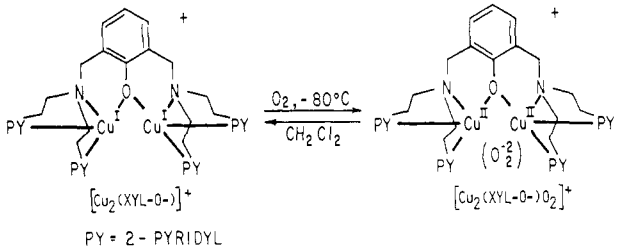

Figure 1. Oxygenation reaction of $[Cu_2(XYL-O-)O_2]^+$.

Laboratories, Woburn, MA) were used without further purification. The solvent (CH_2Cl_2) was obtained from Fisher Scientific Co. and was also used without further purification.

The oxygenated form of the complex $[Cu_2(XYL-O-)O_2]^+$ was prepared by placing the copper(I) precursor into the bottom of a 200-mm quartz EPR tube (3 mm o.d.) which was sealed with a rubber septum. The tube was purged with nitrogen gas for 10 min and then an aliquot of CH_2Cl_2, which had been previously degassed with nitrogen, was injected to dissolve the complex. The purge was maintained while the solution was cooled in a dry ice–acetone bath. After thermal equilibration, the purge was removed and oxygen gas was injected into the solution.

The EPR tube of the resulting $[Cu_2(XYL-O-)O_2]^+$ solution was inserted into a quartz EPR flow dewar insert. The temperature was maintained at −90 °C by flowing cooled nitrogen gas through the dewar insert and controlled with a thermocouple and a Bruker ER 4111 VT variable-temperature unit. The Raman signal was collected through the walls of the dewar insert using a backscattering geometry.

The quartz dewar and sample tube gave an interfering Raman signal in the 500-cm^{-1} region which prevented an accurate determination of the band shape of the metal ligand vibration. To eliminate this quartz interference, the samples were placed in soft-glass NMR tubes, and a soft-glass extension for the dewar insert was constructed.

Resonance Raman spectra were measured on a Spex 1403 double monochromator using a cooled RCA C31034 photomultiplier combined with a Spex digital photometer system and Nicolet 1180E computer.[15] Raman sources included a Coherent CR-18UV argon ion, CR-90K krypton ion, and Rhodamine 6G and Stilbene 3 dye lasers. Typical sample concentrations were 50 mM and laser power was kept at 25–75 mW to minimize sample degradation. The CH_2Cl_2 peaks were used for energy and intensity calibration.

The normal coordinate analysis was based on a Wilson FG matrix method[16] utilizing a modified Urey–Bradley force field. The calculations were performed on an IBM PC AT computer (640K memory), which used a modified Schachtschneider Fortran program.[17,18]

Results and Analysis

An intense violet color develops when dioxygen is added to a light yellow-brown dichloromethane solution of $[Cu_2(XYL-O-)]^+$ at temperatures below −70 °C. This color change has been shown to be associated with a reversible interaction with dioxygen which occurs only at low temperature. If the solution is warmed, the oxygenated derivative irreversibly decomposes to a μ-hydroxy μ-phenoxy copper(II) dimer.[19] The visible absorption spectrum of the violet solution exhibits a strong band at 505 nm with a shoulder at 610 nm (Figure 2). A Gaussian resolution of this spectrum reveals these features to be a strong band at 503 nm (ν_{max} = 19900 cm^{-1}, ϵ = 6300 M^{-1} cm^{-1}) with a weaker component at 625 nm (ν_{max} = 16000 cm^{-1}, ϵ = 1100 M^{-1} cm^{-1}). These spectral features are unique to the violet solution as they do not appear in the spectra of either the copper(I) precursor[19] or the copper(II) decomposition product (Figure 2). An additional

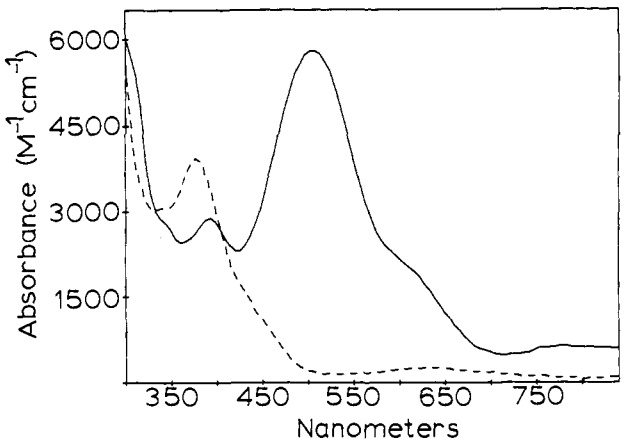

Figure 2. Absorption spectra of $[Cu_2(XYL-O-)O_2]^+$ (—) and $[Cu_2(XYL-O-)OH]^{2+}$ (---).

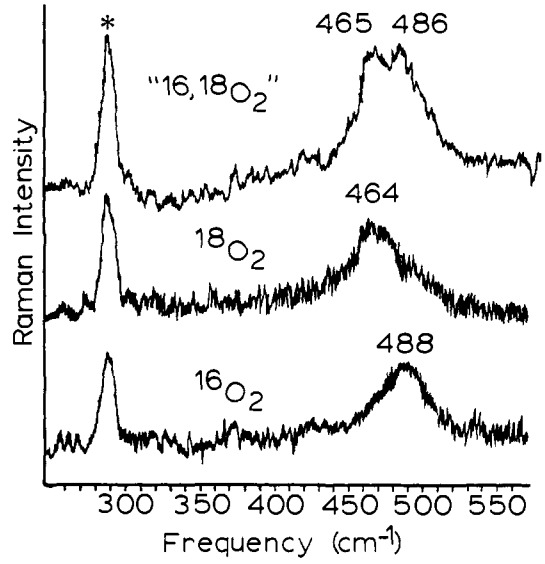

Figure 3. Resonance Raman spectrum of the metal ligand region of $[Cu_2(XYL-O-)O_2]^+$ prepared with $^{16}O_2$, $^{18}O_2$, or "$^{16}O^{18}O$" (the mixture of $^{16}O_2$, $^{18}O_2$, and $^{16}O^{18}O$ described in the text). Note: the peaks indicated by (*) are due to the CH_2Cl_2. Spectral conditions: wavelength, 6471 Å; power at sample, 75 mW; slit width, 8 cm^{-1}; speed, 0.5 cm^{-1}/s; time constant, 0.5 s; computer averaged, sum of 50 scans.

charge-transfer band is observed at ~400 nm. This band does not seem to be related to the peroxide since it is also seen in the decomposed product.[20]

Resonance Raman data have been obtained for the oxygenated complex. The Raman spectrum consists of Raman features at 488 and 803 cm^{-1}.[21] Raman experiments have also been performed on the complex prepared with isotopically labeled dioxygen (99% $^{18}O_2$). Both Raman peaks were observed to shift to lower energy with $^{18}O_2$ substitution; the peak at 488 cm^{-1} moved to 464 cm^{-1} and the peak at 803 to 750 cm^{-1} (Figures 3 and 4). The feature at 803 cm^{-1} in the $^{16}O_2$ complex is composed of two peaks, a main peak at 803 cm^{-1} and a smaller feature at 776 cm^{-1}. However, samples prepared with $^{18}O_2$ do not show a similar lower energy shoulder on the 750-cm^{-1} band. The oxygenated complex was also prepared with dioxygen with a 51 atom % ^{18}O composition. The Raman spectrum of this mixture is a statistical

(15) For further description of Raman system, see: Pate, J. E.; Thamann, T. J.; Solomon, E. I. *Spectrochim. Acta, Part A* **1986**, *42*, 313–318.

(16) (a) McIntosh, D. F.; Michaelian, K. H. *Can. J. Spectrosc.* **1979**, *24*, 1–10. (b) McIntosh, D. F.; Michaelian, K. H. *Ibid.* **1979**, *24*, 35–40. (c) McIntosh, D. F.; Michaelian, K. H. *Ibid.* **1979**, *24*, 65–74.

(17) Schachtschneider, J. H. Technical Report No. 57-65, Shell Development Co., Emeryville, CA 1966.

(18) Fuhres, H.; Kartha, V. B.; Kidd, K. G.; Krueger, P. J.; Mantsch, H. H. Computer Programs for Infrared Spectroscopy, Bulletin No. 15, National Research Council of Canada, 1976.

(19) Karlin, K. D.; Cruse, R. W.; Gultneh, Y.; Hayes, J. C.; McKown, J. W.; Zubieta, J. In ref 9, pp 101–114. (b) Karlin, K. D.; Cruse, R. W.; Gultneh, Y.; Farooq, A.; Hayes, J. C.; Zubieta, J., to be submitted for publication.

(20) This band is probably a phenolate to copper(II) charge-transfer transition based on resonance Raman results for analogous complexes. [See: Pyrz, J. W.; Karlin, K. D.; Sorrell, T. N.; Vogel, G. C.; Que, L., Jr. *Inorg. Chem.* **1984**, *23*, 4581–4584.] However, excitation profiles into this band were not obtained because of laser-induced decomposition of the oxygenated complex at wavelengths <450 nm.

(21) An additional peak appears in the Raman spectrum at ~600 cm^{-1} but its intensity does not appear to correlate with the intensities of the peroxide features and it does not shift on isotopic substitution. No other features were observed in the metal ligand region of the $[Cu_2(XYL-O-)O_2]^+$.

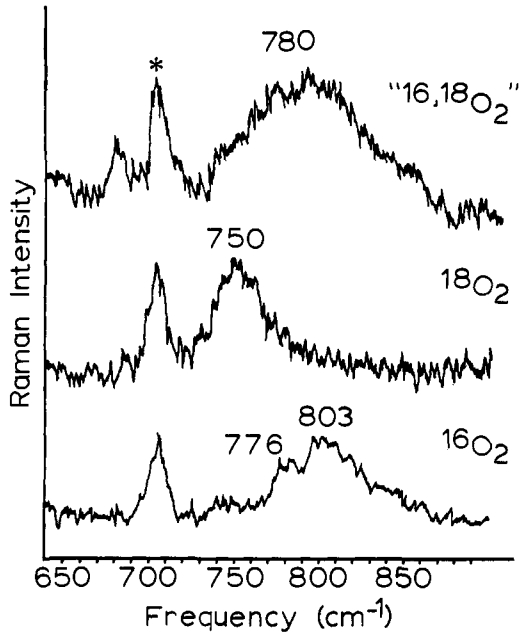

Figure 4. Resonance Raman spectrum of the intraligand region of $[Cu_2(XYL-O-)O_2]^+$ prepared with $^{16}O_2$, $^{18}O_2$, or "$^{16}O^{18}O$" (the mixture of $^{16}O_2$, $^{18}O_2$, and $^{16}O^{18}O$ described in the text). Note: the peaks indicated by (*) are due to the CH_2Cl_2. Spectral conditions: wavelength, 4880 Å; power at sample, 40 mW; slit width, 8 cm^{-1}; speed, 1.0 cm^{-1}/s; time constant, 0.5 s; computer averaged, sum of 10 scans.

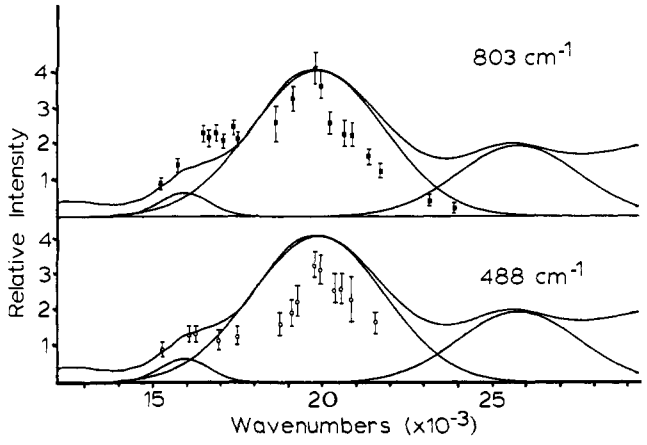

Figure 5. Resonance Raman profile of $[Cu_2(XYL-O-)O_2]^+$. Points of the resonance profile are indicated by O (488-cm^{-1} vibration) and ■ (803 cm^{-1} vibration). The intensities are calculated relative to the CH_2Cl_2 peaks at 285 and 703 cm^{-1}, respectively. The absorption spectrum has been resolved into individual Gaussian components.

combination of $^{18}O_2$, $^{16,18}O_2$, and $^{16}O_2$ with a calculated intensity ratio of 1.08:2.08:1.00, respectively. The experimental ratio from the Raman spectrum was found to be 1.17:2.14:1.00. The Raman spectrum of the oxygenated complex obtained with this isotopic mixture consists of a broad unresolved feature centered at approximately 780 cm^{-1} (Figure 4, top) and a resolved two-component feature (465 and 486 cm^{-1}) in the metal ligand region (Figure 3, top).

Resonance Raman profiles have been obtained for the oxygenated complex (Figure 5) which confirm the assignment of two peroxide to copper(II) charge-transfer features in the optical spectrum. The 803-cm^{-1} vibration is in resonance with both the main absorption band at 503 nm and the 625-nm component. The intensity of the 488-cm^{-1} peak is enhanced from the 503-nm transition but shows less enhancement (relative to the O–O stretch) from the 625-nm shoulder.

The presence of a vibrational peak at 803 cm^{-1} which shifts to 750 cm^{-1} upon isotopic substitution is indicative of dioxygen bound as peroxide. The mixed isotope vibrational data can then be analyzed to determine the mode of peroxide binding in this

Table I. Refinement of $[Cu_2(XYL-O-)O_2]^+$ Isotopic Data to Symmetric and Asymmetric Peroxide Geometries

	$\nu(O-O)_{exptl}$ (cm^{-1})	$\nu(O-O)_{calcd}$ (cm^{-1})	$\nu(Cu-O)_{exptl}$ (cm^{-1})	$\nu(Cu-O)_{calcd}$ (cm^{-1})
				
$^{16}O_2$	803.0	799.1	488.0	487.9
$^{18}O_2$	750.0	753.6	464.0	465.5
$^{16}O^{18}O$		779.1		485.8
$^{18}O^{16}O$		774.5		467.5
		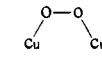		
$^{16}O_2$	803.0	799.4	488.0	486.5
$^{18}O_2$	750.0	754.2	464.0	464.8
$^{16}O^{18}O$		777.4		474.2
$^{18}O^{16}O$		777.4		474.2

K_{O-O} (mdyn/Å)	K_{Cu-O} (mdyn/Å)	H_{Cu-O-O} (mdyn/Å)	F_{Cu-O-O} (mdyn/Å)
			
2.86	1.89	0.217	0.06
	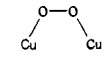		
2.73	2.14	0.132	0.06

R_{O-O} = 1.5 Å, R_{Cu-O} = 1.9 Å, θ_{Cu-O-O} = 115°

complex. A variety of copper peroxide binding geometries is possible, which can be separated into two categories based upon the inequivalence of the oxygen atoms. In the symmetric geometries (μ-1,2 and side-on), the two ends of the peroxide are equivalent and complexes prepared with $^{16,18}O_2$ should exhibit a single oxygen–oxygen stretching frequency. In the asymmetric geometries (μ-1,1 and terminal), the $^{16,18}O_2$ complex should exhibit two different vibrational frequencies depending upon the oxygen isotope bound to the copper(s).

Normal coordinate analyses were performed in order to obtain an approximate value for the isotopic splitting between $^{16}O^{18}O$ and $^{18}O^{16}O$. Two limiting geometries were considered. A monomeric terminal geometry was used as representative of asymmetric copper coordination, and a μ-1,2 geometry was selected for the symmetric case. The geometric parameters used were based on literature values for analogous μ-1,2 cobalt peroxide[12] or terminal cobalt superoxide systems.[22] Since there is a wide range for the cobalt oxygen–oxygen angles in the terminal geometry (118.5–153°), a minimum value of 115° was used. For simplicity of calculation, both geometries were constrained to be planar and only planar motions were considered. A Urey–Bradley force field was chosen in order to minimize the number of force constants (two stretching force constants, K_{O-O}, K_{Cu-O}; a bending force constant, H_{Cu-O-O}; and a repulsion force constant, F_{Cu-O-O}), which were then refined to reproduce the experimental vibrational frequencies (Table I).

The vibrational spectra shown in Figures 6 and 7 were simulated using the results of this frequency calculation combined with the experimental line shapes obtained from the pure $^{18}O_2$ (O–O) or $^{16}O_2$ (Cu–O) data. Since the "$^{16,18}O_2$" is a statistical mixture of $^{16}O_2$, $^{18}O_2$, and $^{16}O^{18}O$, there will be at least three component peaks observed for each vibrational region. In addition, the inequivalence of the two ends of the peroxide in the asymmetric geometry leads to an additional splitting of the frequency of the $^{16}O^{18}O$ component in both the intraligand and the metal ligand regions. This is in contrast to the behavior in the μ-1,2 geometry which exhibits a single vibrational peak in each region due to the $^{16,18}O_2$ species.

The rather large experimental bandwidths used for each component have a significant effect on the shape of the composite

(22) Brown, L. D.; Raymond, K. N. *Inorg. Chem.* **1975**, *14*, 2595–2601 and references contained therein.

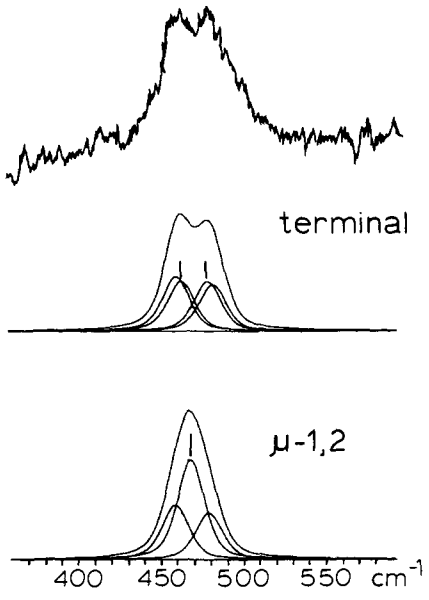

Figure 6. Comparison of the resonance Raman spectrum of the copper peroxide stretch prepared with the "$^{16,18}O_2$" mixture and the band shapes generated by a normal coordinate analysis for peroxide bound in a terminal or μ-1,2 geometry (details given in Table I). The features indicated by a solid vertical line are the components from the $^{16}O^{18}O$ species.

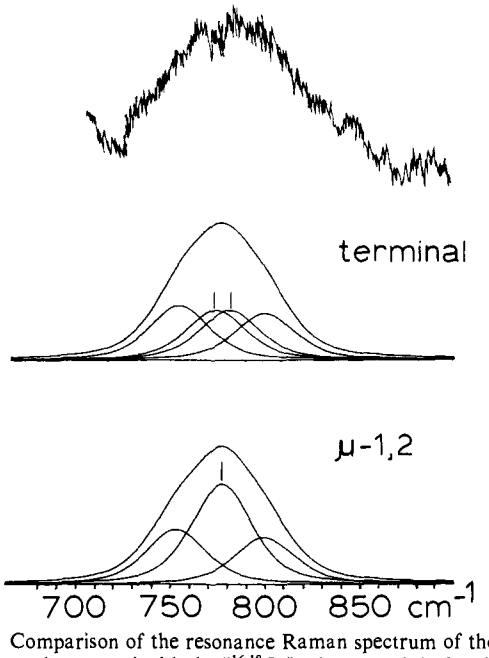

Figure 7. Comparison of the resonance Raman spectrum of the intraperoxide stretch prepared with the "$^{16,18}O_2$" mixture and the band shapes generated by a normal coordinate analysis for peroxide bound in a terminal or μ-1,2 geometry (details given in Table I). The features indicated by a solid vertical line are the components from the $^{16}O^{18}O$ species.

simulation. In the case of the intraperoxide stretch, the band shapes of the calculated spectra for both geometries are indistinguishable. However, the simulated metal ligand band shapes are quite different. The two peaked appearance of the copper peroxide vibrational feature at the top of Figure 6 thus demonstrates an asymmetric peroxide geometry (either terminal or μ-1,1). EXAFS results further indicate a terminal peroxide geometry[23,24] (vide infra).

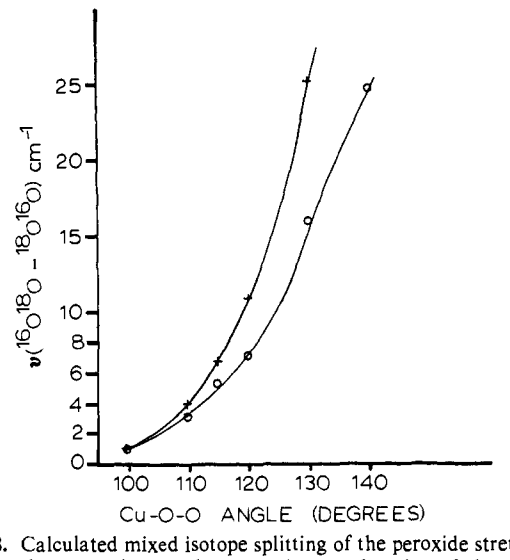

Figure 8. Calculated mixed isotope splitting of the peroxide stretching frequency for a terminal oxyhemocyanin as a function of the copper peroxide angle. The copper peroxide bending frequency ($\delta_{Cu\text{-}^{16}O\text{-}^{16}O}$) used was 170 cm^{-1}.[30] Points denoted by O were calculated for a copper of mass 63.54 (both with the peroxide protonated or unprotonated) and points indicated by + for a copper of mass 10000. (See text for details of calculation.)

From these experiments, values are now known for the intraligand and copper ligand vibrational frequencies for peroxide bound asymmetrically to one copper. The problem of whether a <3-cm^{-1} splitting would be too small for a terminal peroxide geometry (vide supra) can then be addressed through normal coordinate calculations. Four different undefined parameters can affect the mixed isotope splitting. These parameters are the copper peroxide angle, the magnitude of the copper peroxide bending frequency, the magnitude of the copper peroxide stretching frequency (in oxyhemocyanin as compared to $[Cu_2(XYL\text{-}O\text{-})O_2]^+$), and off-diagonal interaction force constants in the Urey–Bradley force field (specifically the interaction between the copper–oxygen stretch and the oxygen–oxygen stretch). For each parameter, three different sets of calculations were performed: (1) the copper mass was set at 63.54, (2) the copper mass was made arbitrarily large (10000), and (3) a proton was bound to the peroxide with the same parameters as in hydrogen peroxide[25] (copper mass equal to 63.54).

Each calculation was performed by considering a three-body problem, consisting of a copper and two oxygens in a terminal geometry. The copper–peroxide and O–O bond lengths were obtained from μ-1,2 peroxy cobalt complexes.[12] Three normal coordinates were included (two stretches and a bend) and four (or five) force constants were used [$K_{O\text{-}O}$, $K_{Cu\text{-}O}$, $H_{Cu\text{-}O\text{-}O}$, and $F_{Cu\text{-}O\text{-}O}$ (with $K_{off\text{-}diag}$ added for the final set of calculations)]. For the protonated case, another internal mode, the OH stretch (with the associated $K_{O\text{-}H}$), was added. The force field was then refined to the $^{16}O_2$ and $^{18}O_2$ isotopic peroxide stretching frequencies obtained for oxyhemocyanin (749 and 708 cm^{-1} [2a]) and the $^{16}O_2$ and $^{18}O_2$ copper peroxide stretching frequencies from $[Cu_2(XYL\text{-}O\text{-})O_2]^+$. Since there are more force constants than independent vibrational frequencies, there will not be a unique solution to the refinement. For each calculation, limits were placed on $F_{Cu\text{-}O\text{-}O}$ by considering a series of fixed values for $F_{Cu\text{-}O\text{-}O}$, ranging from zero to a maximum value such that the bending force constant, $H_{Cu\text{-}O\text{-}O}$, remained greater than the repulsion force constant, $F_{Cu\text{-}O\text{-}O}$. The value for $F_{Cu\text{-}O\text{-}O}$ which gave the smallest calculated mixed isotope splitting was used in constructing Figures 8–11.

A final set of calculations has been performed to estimate the effects of going from the terminal monomer to the cis μ-1,2 dimer, which is the spectroscopically predicted geometry for oxyhemo-

(23) Blackburn, N. J.; Strange, R. W.; Cruse, R. W.; Karlin, K. D. *J. Am. Chem. Soc.*, submitted for publication.

(24) (a) Karlin, K. D.; Hayes, J. C.; Gultneh, Y.; Cruse, R. W.; McKown, J. W.; Hutchinson, J. P.; Zubieta, J. *J. Am. Chem. Soc.* **1984**, *106*, 2121–2128. (b) Karlin, K. D.; Dahlstrom, P. L.; Cozzette, S. N.; Scensy, P. M.; Zubieta, J. *J. Chem. Soc., Chem. Commun.* **1981**, 881–882. (c) Sorrell, T. M.; Jameson, D. L.; O'Connor, C. J. *Inorg. Chem.* **1984**, *23*, 190–195.

(25) Redington, R. C.; Olson, W. B.; Cross, P. C. *J. Chem. Phys.* **1962**, *36*, 1311–1326.

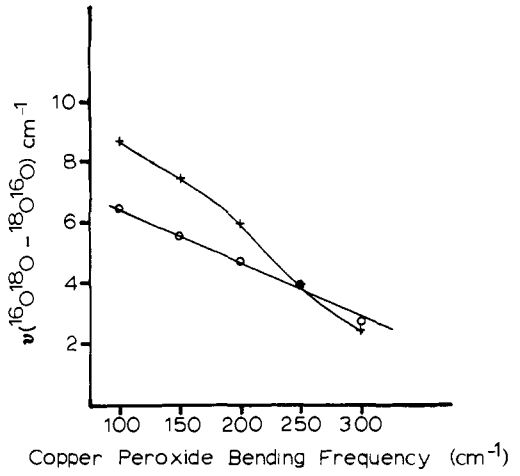

Figure 9. Calculated mixed isotope splitting of the peroxide stretching frequency for a terminal oxyhemocyanin as a function of the copper peroxide bending frequency. A copper peroxide angle of 115° was used. Points denoted by O were calculated for a copper of mass 63.54 (both with the peroxide protonated or unprotonated) and points indicated by + for a copper of mass 10 000.

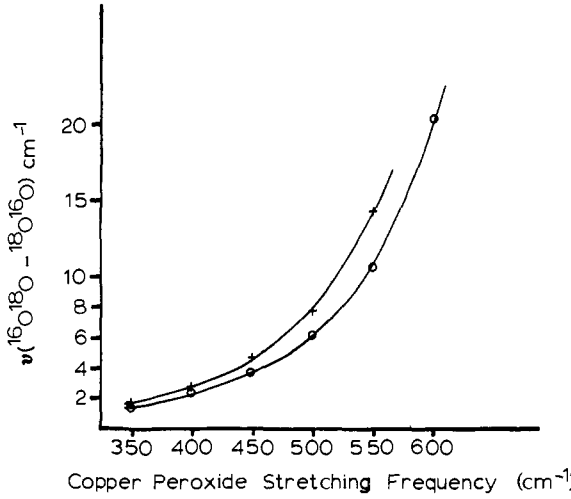

Figure 10. Calculated mixed isotope splitting of the peroxide stretching frequency for a terminal oxyhemocyanin as a function of the copper peroxide stretching frequency. A copper peroxide angle of 115° and a copper peroxide bending frequency ($\delta_{Cu-^{16}O-^{16}O}$) of 170 cm^{-1} were used.[30] Points denoted by O were calculated for a copper of mass 63.54 (both with the peroxide protonated or unprotonated) and points indicated by + for a copper of mass 10 000.

cyanin. These calculations were performed in two parts. First, a cis μ-1,2 geometry was constructed by taking the terminal geometry and adding a symmetrically equivalent copper to the free end of the peroxide. The force field obtained from the experimental frequencies of $[Cu_2(XYL-O-)O_2]^+$ (Table I, terminal geometry) was then directly applied to this geometry. The energy levels obtained on going from the monomer to the dimer are presented in Figure 12. Second, in order to predict the copper peroxide stretching frequencies by oxyhemocyanin in the cis μ-1,2 geometry, a calculation has been performed in which the peroxide stretching frequency of oxyhemocyanin was combined with the copper peroxide stretching force constant from $[Cu_2(XYL-O-)O_2]^+$ and the Cu–O–O bending frequency of 170 cm^{-1} obtained from a peroxy cobalt complex (vide infra). The copper peroxide force constant was kept fixed and the rest of the force field was allowed to refine. The predicted values of the symmetric and asymmetric copper peroxide stretching frequencies are given in Table II.

Discussion

There have been several studies using mixed isotopes to determine the geometry of dioxygen binding in structurally un-

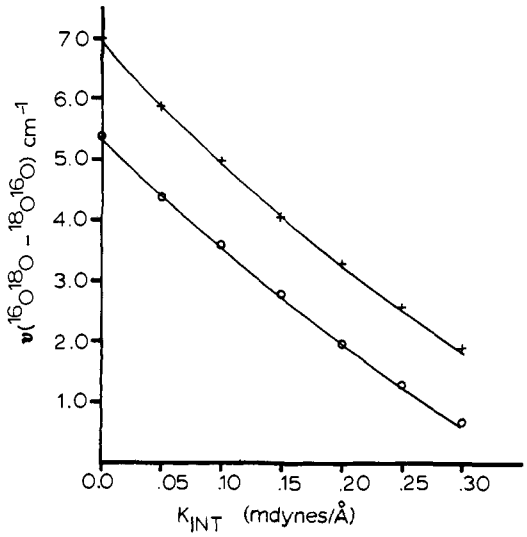

Figure 11. Calculated mixed isotope splitting of the peroxide stretching frequency for a terminal oxyhemocyanin as a function of the off-diagonal stretch–stretch interaction force constant. A copper peroxide angle of 115° and a copper peroxide bending frequency ($\delta_{Cu-^{16}O-^{16}O}$) of 170 cm^{-1} were used.[30] Points denoted by O were calculated for a copper of mass 63.54 (both with the peroxide protonated or unprotonated) and points indicated by + for a copper of mass 10 000.

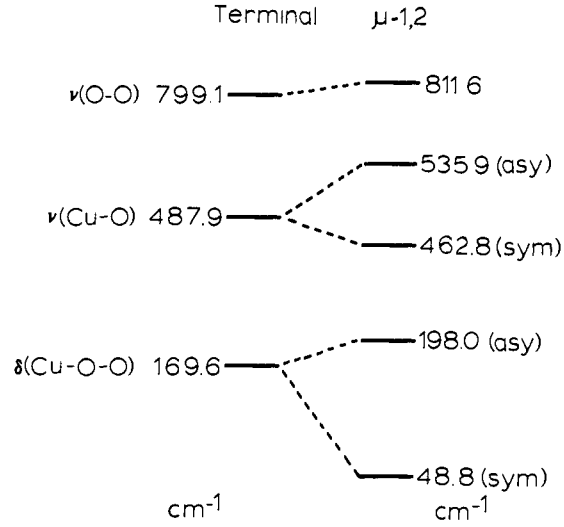

Figure 12. Comparison of the vibrational frequencies of a copper peroxide system calculated from equivalent force constants (given in Table II) in the terminal monomer and cis μ-1,2 geometries.

Table II. Calculated Symmetric and Asymmetric Copper Peroxide Stretching Frequencies of Oxyhemocyanin Using the Copper Peroxide Stretching Force Constant from $[Cu_2(XYL-O-)O_2]^+$ and the Intraperoxide Stretching Frequency from Oxyhemocyanin

O—O / Cu Cu	ν(O–O)$_{init.}$ (cm^{-1})	ν(O–O)$_{calcd}$ (cm^{-1})	ν(Cu–O)$_{calcd}$ (sym) (cm^{-1})	ν(Cu–O)$_{calcd}$ (sym) (cm^{-1})
$^{16}O_2$	749.0	750.3	530.1	453.6
$^{18}O_2$	708.0	707.9	504.8	433.2

K_{O-O} (mdyn/Å)	K_{Cu-O} (mdyn/Å)	H_{Cu-O-O} (mdyn/Å)	F_{Cu-O-O} (mdyn/Å)
2.41	1.89	0.196	0.008

characterized complexes.[26-28] In most of these studies, only the intraligand vibration was investigated and the lack of an observable

(26) (a) Shibahara, T.; Mori, M. *Bull. Chem. Soc. Jpn.* **1978**, *51*, 1374–1379. (b) Kurtz, D. M., Jr.; Shriver, D. F.; Klotz, I. M. *J. Am. Chem. Soc.* **1976**, *98*, 5033–5035. (c) Nakamura, A.; Tatsuno, Y.; Yamamoto, M.; Otsuka, S. *Ibid.* **1971**, *93*, 6052–6058.

(27) (a) Kozuka, M.; Nakamoto, K. *J. Am. Chem. Soc.* **1981**, *103*, 2162–2168. (b) McIntosh, D.; Ozin, G. A. *Inorg. Chem.* **1976**, *15*, 2869–2871.

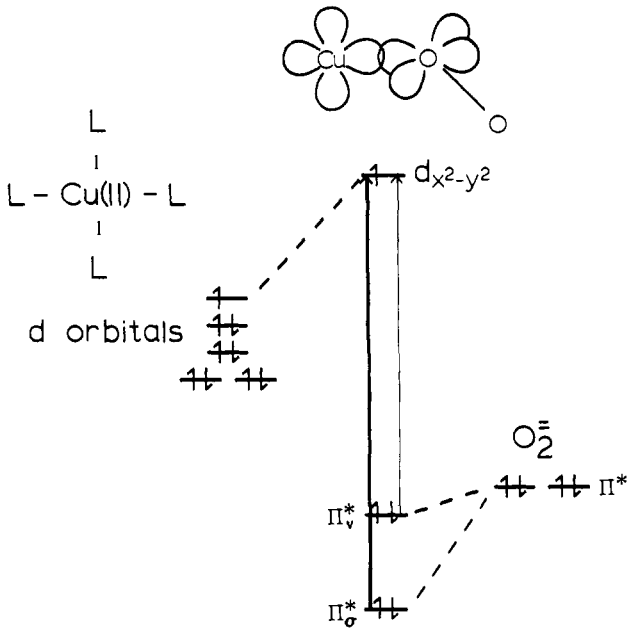

Figure 13. Energy level diagram of the molecular orbitals participating in the copper–peroxide bond in a Cu–O–O monomer.

isotopic splitting was interpreted to indicate that the dioxygen was bound in a symmetric geometry. In the case of $[Cu_2(XYL\text{-}O\text{-})O_2]^+$, the bandwidths are too broad to lead to a resolved isotopic splitting even if the $^{16,18}O_2$ components are split by as much as 6–10 cm^{-1} (Figure 7). The copper peroxide peak (Figure 6), however, exhibits a pronounced difference in the predicted isotopic band shape for the two geometries. This results from the narrower component bandwidth [38 cm^{-1} (O–O) vs. 19.5 cm^{-1} (Cu–O)] and the larger calculated mixed isotope splitting [4.6 cm^{-1} (O–O) vs. 18.3 cm^{-1} (Cu–O)]. The two-peaked appearance of the copper peroxide stretch in Figure 3 requires that the peroxide is bound in an asymmetric geometry. Recent EXAFS results have indicated a 3.31-Å copper–copper distance for $[Cu_2(XYL\text{-}O\text{-})O_2]^+$.[23] This result rules out the μ-1,1 bridging geometry, since existing structural data for phenoxide plus OH^- or OMe^- doubly bridged complexes with similar ligands show that a μ-1,1 geometry is only compatible with a copper–copper distance of less than 3.15 Å.[24] However, a terminal geometry would require that the peroxide is coordinatively unsaturated. Steric considerations do suggest that the free end of the peroxide could be stabilized by a weaker axial interaction with the second copper, and molecular models indicate that the 3.31-Å copper–copper distance would be compatible with a μ-1,2 equatorial to axial peroxide geometry. However, even if an axial interaction is present, the mixed isotope results indicate a peroxide geometry that is essentially terminal in character.

Thus, the spectral features of peroxide bound to copper(II) in a terminal geometry can now be developed. The intraligand stretching frequency at 803 cm^{-1} and its shift to 750 cm^{-1} upon substitution with $^{18}O_2$ are very similar to the peroxide stretching frequencies observed for peroxy cobalt complexes.[12,13] The Raman peak at 488 cm^{-1} (464 cm^{-1}, $^{18}O_2$) can be identified as the copper peroxide stretching frequency based on its behavior upon isotopic substitution, thus providing an estimate of the strength of the copper peroxide interaction. The resonance Raman enhancement profiles indicate that two absorption bands can be assigned as peroxide to copper(II) charge-transfer transitions: an intense peak at 503 nm (ϵ = 6300 M^{-1} cm^{-1}) and a weaker band at 625 nm (ϵ = 1100 M^{-1} cm^{-1}). The intraligand vibration at 803 cm^{-1} is in resonance with both peroxide to copper(II) charge-transfer transitions while the intensity of the metal ligand peak at 488 cm^{-1} exhibits enhancement primarily from the 503-nm band.

The charge-transfer spectrum of the $[Cu_2(XYL\text{-}O\text{-})O_2]^+$ complex can be interpreted by considering the bonding properties of a copper(II) peroxide monomer (Figure 13). The highest energy occupied orbitals of the peroxide are a degenerate π^* set which split in energy upon binding to the copper. One π^* orbital (π^*_σ) forms a σ bond to the $d_{x^2-y^2}$ orbital of the copper and is strongly stabilized by this interaction. The other π^* orbital (π^*_v) is perpendicular to the copper $d_{x^2-y^2}$ plane and undergoes a weaker π-bonding interaction. Thus, two peroxide-to-copper(II) charge-transfer transitions result from this scheme. The π^*_σ transition should be at higher energy owing to its greater stabilization and should have greater intensity than the π^*_v transition because of its larger overlap with the copper $d_{x^2-y^2}$ orbital. The two peroxide π^* charge-transfer transitions should also exhibit different resonance Raman behavior. Since the π^*_v orbital is weakly π bonding to the copper, removal of an electron from this orbital should primarily result in a distortion along the oxygen–oxygen coordinate and therefore the major enhancement should be observed in the intraperoxide stretch. However, removal of an electron from the π^*_σ should cause distortions along both the oxygen–oxygen and the copper peroxide coordinates, since the π^*_σ orbital is σ bonding with respect to the copper as well as antibonding with respect to the peroxide. This should result in resonance enhancement of both the copper peroxide and intraperoxide stretching modes. The resonance Raman behavior combined with the higher energy and intensity of the 503-nm band lead to its assignment as the π^*_σ charge-transfer transition. Analogously, the 625-nm shoulder is assigned as the π^*_v charge-transfer transition.

A Gaussian resolution of the absorption spectrum of $[Cu_2(XYL\text{-}O\text{-})O_2]^+$ indicates that the π^*_σ–π^*_v splitting is ~4000 cm^{-1}. The oscillator strength, f, for the π^*_σ transition is approximately 0.13 (for the π^*_v transition f = 0.009). In comparison, oxyhemocyanin exhibits two features in the optical absorption spectrum [a band at 345 nm (ϵ = 20000 M^{-1} cm^{-1}, f = 0.4) and a lower energy feature at 580 nm (ϵ = 1000 M^{-1} cm^{-1}, f = 0.02)], and an additional circular dichroism peak [near 480 nm ($\Delta\epsilon$ ~ 2 M^{-1} cm^{-1})]. The greater intensity and higher energy of the 345-nm absorption in oxyhemocyanin indicates that this band must be a π^*_σ charge-transfer transition. The 580-nm absorption band has been similarly assigned as a π^*_v transition, thus for oxyhemocyanin the π^*_σ–π^*_v splitting is 12000 cm^{-1}. The presence of three charge-transfer transitions indicates a bridging peroxide geometry in oxyhemocyanin, since a terminally bound peroxide geometry can have only two charge-transfer transitions.[3] If the peroxide bridges two copper(II)'s then four charge-transfer transitions should result: the symmetric and antisymmetric combinations of each of the π^*_σ and π^*_v peroxide to copper(II) charge-transfer transitions. The higher intensities and energy splittings of the charge-transfer features in oxyhemocyanin as compared to $[Cu_2(XYL\text{-}O\text{-})O_2]^+$ are also consistent with peroxide being bound to an additional copper in the protein. Both the oscillator strengths and the π^*_σ–π^*_v splitting would be expected to increase because of additional overlap and stabilization of the π^*_σ orbital upon binding to the second copper ion.

The lack of a mixed isotope splitting for oxyhemocyanin can be further considered using normal coordinate analyses, as a value of the copper peroxide force constant has been obtained from this model complex. Four undefined factors can affect the mixed isotope splitting, and each has been systematically varied in order to estimate a minimum value of this splitting for an asymmetric peroxide geometry. These normal coordinate calculations indicate that a copper peroxide angle of less than 110°, a copper peroxide bending frequency greater than 275 cm^{-1}, a copper peroxide stretching frequency less than 425 cm^{-1}, or an off-diagonal interaction force constant of K_{int} > 0.13 mdyn/Å would be necessary to give a mixed isotope splitting less than the 3-cm^{-1} resolution limit.

Each of these factors, considered individually, is probably not enough to prevent resolution of the mixed isotope splitting. First, an estimate of a terminal copper peroxide angle can be obtained

(28) (a) Huber, H.; Klotzbucher, G. A.; Ozin, G. A.; Vander Voet, A. *Can. J. Chem.* **1973**, *51*, 2722–2736. (b) Andrews, L. *J. Chem. Phys.* **1969**, *50*, 4288–4299.

by considering the Co–O–O angles in both the terminal cobalt superoxide (118.5–153°)[22] and the monobridged binuclear cobalt peroxide complexes (110–120°).[12] Second, while there has been little work done in identifying the metal dioxygen bending frequencies in transition metal peroxide complexes, the symmetric cobalt peroxide bending frequency of 174 cm^{-1} has been confirmed by $^{18}O_2$ isotopic substitution[29] in μ-1,2 $K_6[(CN)_5CoO_2Co(CN)_5]\cdot H_2O$. Third, a copper peroxide stretching frequency has been observed in this study at 488 cm^{-1} for the $[Cu_2(XYL\text{–}O\text{–})O_2]^+$ complex. Finally, an estimate for interaction force constants is difficult to obtain.[31] For side-on peroxo complexes, this interaction force constant can become quite large ($K_{int} > 0.45$ mdyn/Å).[28a] However, there should be much more coupling of the vibrational modes in this case as compared to a terminal geometry. Normal coordinate calculations of μ-1,2 metal peroxide complexes[26a,29] have not included interaction force constants, but the mixed isotope splittings were not specifically investigated. In oxyhemerythrin, which contains a terminally bound peroxide, $^{16}O^{18}O$ data have been obtained.[26b] The mixed isotope results were interpreted using a normal coordinate analysis which did not require the addition of an interaction force constant to reproduce the observed 5–7-cm^{-1} splitting. Although combinations of the above parameters would be able to sufficiently lower the mixed isotope splitting to prevent resolution of the components, it appears likely that if the peroxide binds terminally in oxyhemocyanin, the mixed isotope splitting would be large enough to be observed.

A comparison of the resonance Raman spectral features of oxyhemocyanin with $[Cu_2(XYL\text{–}O\text{–})O_2]^+$ reveals several significant differences. The peroxide stretching frequency is much lower in oxyhemocyanin (749 vs. 803 cm^{-1}). A calculation was done to determine whether this lower frequency could result from the mechanical contribution of adding a second copper to form a cis μ-1,2 dimer. Using the force field of the monomer, addition of the second copper causes the peroxide stretching frequency to go up in the dimer (Figure 12). Therefore, the lower peroxide stretching frequency in oxyhemocyanin is not due to a mechanical effect but appears to relate to a weaker oxygen–oxygen bond (i.e., a smaller oxygen–oxygen force constant, 2.86 vs. 2.41 mdyn/Å). Consideration of the energy levels in hydrogen peroxide indicates that the π, as well as the π^* orbitals, can participate in bonding to the hydrogens.[32] Mixing of the π bonding orbitals with the valence orbitals of the two copper(II)'s would weaken the intraperoxide bond. Calculations of the bonding interactions of the peroxide energy levels with the coppers are necessary to evaluate this possibility.[33]

The resonance Raman profiles of the peroxide stretching frequency in $[Cu_2(XYL\text{–}O\text{–})O_2]^+$ are also different relative to those of oxyhemocyanin. In $[Cu_2(XYL\text{–}O\text{–})O_2]^+$, the degree of enhancement of the O–O peak is greater from the π^*_σ band compared to the π^*_v feature. Oxyhemocyanin, however, shows a similar intensity enhancement of the intraperoxide stretch from both the π^*_v and the very intense π^*_σ bands. The resonant behavior of the copper peroxide mode, in particular, shows significant differences between these two systems. In the terminal model complex, the copper peroxide vibration shows significantly more enhancement from the π^*_σ charge-transfer band compared to the π^*_v charge-transfer shoulder. The lack of other observed metal ligand modes in the 200–500-cm^{-1} region in the resonance Raman spectrum indicates that the copper peroxide stretch is the dominant metal ligand mode enhanced in both the π^*_σ and π^*_v transitions. On forming the μ-1,2 dimer in oxyhemocyanin, the copper peroxide frequency would split into two components, an asymmetric and symmetric stretch. By assuming a similar $K_{Cu\text{–}O}$ in both systems, the totally symmetric stretching frequency is predicted to be at about 453 cm^{-1} (Table II). However, a resonance-enhanced copper peroxide mode has not been observed in this energy region in oxyhemocyanin.[2] Instead, the intensities of the copper imidazole modes at ~270 cm^{-1} show a large enhancement from the 345-nm band[2a] and appear to exhibit limited enhancement from the 580-nm transition.[2b] As mechanical coupling can now be neglected, these differences in the resonance Raman profiles between oxyhemocyanin and $[Cu_2(XYL\text{–}O\text{–})O_2]^+$ may relate to differences in the excited-state distortions associated with the charge-transfer transitions in the bridged dimer structure. This possibility, however, requires further spectroscopic study on a structurally defined peroxide-bridged binuclear metal complex.

Acknowledgment. We thank the National Institutes of Health, Grants AM31450 (E.I.S.) and GM28962 (K.D.K.), for support of this research.

(29) Hester, R. E.; Nour, E. M. *J. Raman Spectrosc.* **1981**, *11*, 45–48.
(30) From a normal coordinate calculation of the vibrational data of μ-1,2-$K_6[(CN)_5CoO_2Co(CN)_5]\cdot H_2O$,[29] it was determined that the symmetric and asymmetric bending frequencies should be split by ~10 cm^{-1}. Therefore, an intermediate value of 170 cm^{-1} was used for the terminal geometry.
(31) Shimanouchi, T. *Pure Appl. Chem.* **1963**, *7*, 131–145.
(32) Kaldor, U.; Shavitt, I. *J. Chem. Phys.* **1966**, *44*, 1823–1829.
(33) Other factors which could also contribute to the reduced O–O stretching frequency in oxyhemocyanin are hydrogen bonding, hydrophobicity, or possible electrostatic interactions in the active site. See: Loehr, J. S.; Freedman, T. B.; Loehr, T. M. *Biochem. Biophys. Res. Commun.* **1974**, *56*, 510–515.